

Onset of Chaos in Rapidly Rotating Nuclei

Sven Åberg

*Joint Institute for Heavy Ion Research, Holifield Heavy Ion Research Facility, Oak Ridge, Tennessee 37831
and Department of Mathematical Physics, Lund Institute of Technology, P.O. Box 118, S-22100 Lund, Sweden^(a)*

(Received 14 August 1989)

The onset of chaos is investigated for excited, rapidly rotating nuclei, utilizing a schematic two-body residual interaction added to the cranked Nilsson Hamiltonian. Dynamical effects at various degrees of mixing between regularity and chaos are studied in terms of fragmentation of the collective rotational strength. It is found that the onset of chaos is connected to a saturation of the average standard deviation of the rotational strength function. Still, the rotational-damping width may exhibit motional narrowing in the chaotic regime.

PACS numbers: 24.60.Ky, 05.45.+b

Studying how a quantum-mechanical system behaves when the corresponding classical system changes from regular to a chaotic behavior is a subject of great current interest. The nuclear many-body problem may then be a particularly interesting case. While a severe suppression of dynamical effects takes place in low-dimensional quantum-mechanical systems, as compared to the corresponding classical chaotic systems, quantum systems with higher dimensions seem to behave more similar to the corresponding classical one. For example, diffusion of the momenta is severely suppressed in one kicked rotor¹ while the momenta diffuse much more classical-like in a system consisting of two sufficiently strongly coupled rotors.² One might therefore expect that the many coupled nucleons in the atomic nucleus (in some respect) exhibit chaos³ in a more classical-like way.

It would be most interesting if one could study experimentally the onset of chaos in the nucleus. At present, it is hardly possible to measure all discrete energy states, with assigned spin and parity, the first few MeV above the yrast line and study the level statistics. Instead, one may look for other variables. An important question is then how the onset of chaos affects different *measurable* observables, static as well as dynamical. In this Letter we shall discuss how the onset of chaos in rapidly rotating nuclei affects particularly the strength function for collective $E2$ transitions.

To address these questions we study the Hamiltonian

$$H = H_1 + H_{\text{res}}, \quad (1)$$

consisting of a one-body part H_1 and a residual interaction H_{res} . The pairing interaction is believed to be of minor importance and is therefore ignored. The one-body part is obtained in a microscopic way from the cranked Nilsson model,⁴ $h = h_{\text{Nilsson}}(\epsilon, \epsilon_4, \gamma) - \omega j_x$. The cranked ground state $|0, \omega\rangle$ is calculated at the appropriate, self-consistent minimum deformation, ϵ , ϵ_4 , and γ , and at the rotational frequency ω corresponding to the desired spin value I_0 . This "ground state" of the nucleus may thus be a yrast state or a shape-isomeric high-spin state. Excited states are obtained at the fixed deforma-

tion as many-particle-many-hole (np - nh) excitations:

$$|\mu, \omega\rangle = \prod_{i=1}^n a_{m_i}^\dagger a_{j_i} |0, \omega\rangle. \quad (2)$$

The corresponding energies, angular momenta, and moments of inertia are simple additive quantities:

$$E_\mu(\omega) = E_0 + \sum_{i=1}^n (e_{m_i} - e_{j_i}),$$

$$I_\mu = I_0 + \sum_{i=1}^n (j_{m_i} - j_{j_i}), \quad \mathcal{J}_\mu^{(1)} = \frac{I_\mu}{\omega},$$

where e_m (e_j) and j_m (j_j) are energies and angular momenta, respectively, of single-particle (-hole) states. In the same way the parity and the signature are obtained for each excited state. The second-derivative moment of inertia is numerically calculated as $\mathcal{J}_\mu^{(2)} = \Delta I_\mu / \Delta \omega$. Finally, the energy for a given spin value is calculated by extrapolation along the rotational band:

$$E_\mu(I) = E_\mu(\omega) + \frac{I_\mu(I - I_\mu)}{\mathcal{J}_\mu^{(1)}} + \frac{(I - I_\mu)^2}{2\mathcal{J}_\mu^{(2)}}. \quad (3)$$

Since the deformation is kept fixed, all the states (2) are orthogonal. A drawback of keeping the deformation constant is, however, that the excited states are not *self-consistent* solutions to H_1 . To minimize this deficiency we shall only study nuclei with deep and stable potential-energy minima. The two cases considered here, ¹⁶⁸Yb at $\epsilon=0.25$ and ¹⁵²Dy at $\epsilon=0.58$ (2:1 deformation), obey this criterion.⁵

By Eq. (3) we have performed a transformation from a system with constant rotational frequency and dispersion in angular momentum, to the physically more realistic system with constant angular momentum but with dispersion in rotational frequency σ_ω . This dispersion is shown in Fig. 1 for the two considered cases. The qualitative behavior can be quite well described by the analytical estimate by Lauritzen, Døssing, and Broglia,⁶ $\sigma_\omega \propto E_{\text{exc}}^{1/4} I / \epsilon$, though this result was obtained for the pure harmonic oscillator with its unrealistic alignment properties.

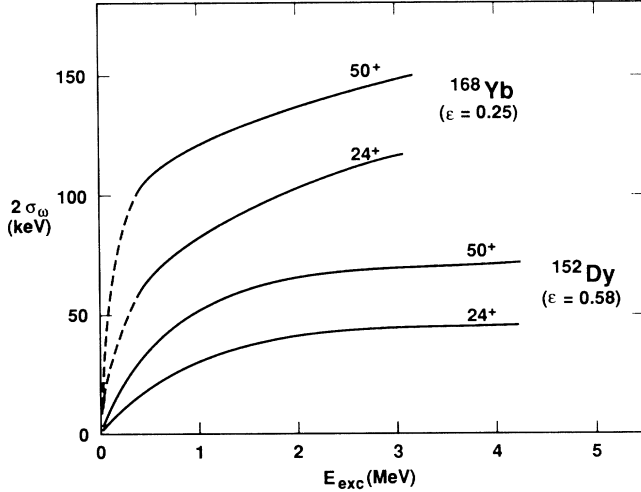


FIG. 1. Dispersion in rotational frequency vs excitation energy above the yrast state E_{exc} for ^{168}Yb ($\epsilon=0.25$) and ^{152}Dy ($\epsilon=0.58$), at spin $I^\pi=24^+$ and 50^+ .

Figure 2 shows the average energy distance between 2p-2h neighboring states \bar{d}_{2p-2h} ($=1/\bar{\rho}_{2p-2h}$), at spin 50^+ as a function of the excitation energy. Only the one-body part of the Hamiltonian is included. Because of the large negative shell energy, particularly for the superdeformed ^{152}Dy , the average level distance is quite large. Since chaos is expected to set in when the average level distance is of the order of the coupling matrix element,⁷ one may expect chaos to set in at a considerably higher excitation energy for the superdeformed ^{152}Dy than for the normal-deformed ^{168}Yb , providing the two-body coupling strength has a similar size in the two cases.

Next we add the residual interaction. The significant part of $H_{\text{res}}=H_2+H_3$ is the two-body part,

$$H_2 = \frac{1}{4} \sum_{m_1 m_2 j_1 j_2} V_2(m_1, m_2, j_1, j_2) \times [a_{m_1}^\dagger a_{m_2}^\dagger a_{j_1} a_{j_2}]_{I=0, \pi=+, a=0}.$$

In the present calculations we assume all matrix elements to have the same absolute value, $V_2 = \pm \Delta$, where Δ is treated as a parameter, and the sign is chosen randomly in order to avoid coherent effects.⁸ The three-body force is included in order to account for truncation effects. Its strength is, rather arbitrarily, taken to be $V_3 = \pm 0.001\Delta$. The diagonalization is performed including the lowest 500 states at given spin (thus given signature) and parity. These states cover the energy region 0–3.6 and 0–2.3 MeV above the yrast state in the superdeformed ^{152}Dy and the normal-deformed ^{168}Yb , respectively (for $I^\pi=50^+$).

One of the aims is to study the system at various excitation energies. However, due to computational limitations excitation energies above ~ 3.5 MeV cannot be studied. Instead one may utilize an approximative scaling property of the system. The states resulting from the

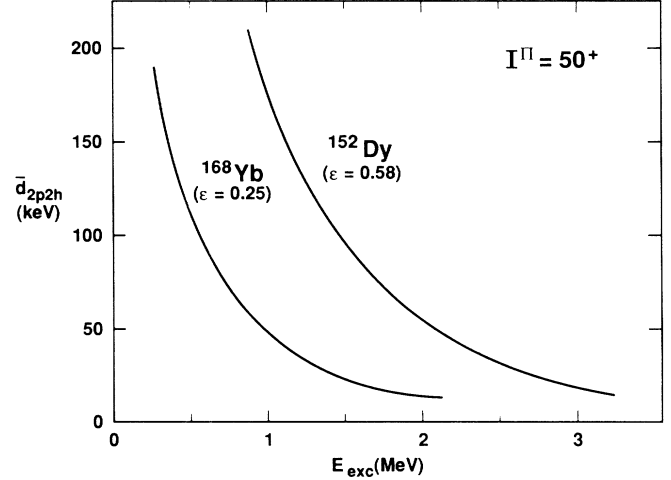


FIG. 2. Average energy distance between 2p-2h neighboring rotational bands vs excitation energy at $I^\pi=50^+$.

diagonalization of Eq. (1) mix over an energy region of unperturbed states Γ_μ that is rather well described by Fermi's "golden rule," $\Gamma_\mu = 2\pi\Delta^2\rho_{2p-2h}(E_{\text{exc}})$; i.e., an increase of the coupling length is obtained either by an increase in Δ or in E_{exc} . In the Fermi-gas model the level density of 2p-2h neighbors is $\rho_{2p-2h} \propto E_{\text{exc}}^{3/2}$.⁶ We may thus study the system at the "scaled" energy $s = \Delta^2 \times E_{\text{exc}}^{3/2}$,⁹ and an increase of the excitation energy can be approximately simulated by an increase in the strength of the two-body interaction Δ in such a way that s is kept constant. The study may then be performed at energy intervals where the level statistics is good. Although this procedure presumably does not account for all possible excitation-energy effects, it is simple and feasible for numerical calculations.

After unfolding the spectrum by a Strutinsky type of smearing procedure, various fluctuation properties are studied.¹⁰ In Fig. 3 the Δ_3 statistics is shown for ^{152}Dy at $I^\pi=50^+$ and $E_{\text{exc}}=3\text{--}3.5$ MeV for different values of the strength of the residual interaction. As a comparison the Δ_3 behavior for Poisson and Gaussian-orthogonal-ensemble (GOE) fluctuations are shown. Note how the curves smoothly change from Poisson to GOE as Δ increases. For large- Δ values the fluctuations follow the GOE behavior also for large- L values, and there is no tendency for deviations from the generic behavior, that has been reported, e.g., for the H atom in a strong magnetic field,¹¹ and for a model calculation by Guhr and Weidenmüller.⁷ In the H-atom case the deviations can be understood in terms of short periodic orbits.¹¹ In the present nuclear case we hardly expect deviations from the generic behavior due to periodic orbits. This may be seen from the estimate $L_{\text{max}} = \bar{\rho}h/T_{\text{min}} \sim 80A^{-1/3}\bar{\rho}_{\text{tot}} \sim 8000$, for the case studied in Fig. 3. The deviations from generic behavior at large- L values obtained in Ref. 7 were explained as due to a limited extension of the wave function. The size of the wave function's localiza-

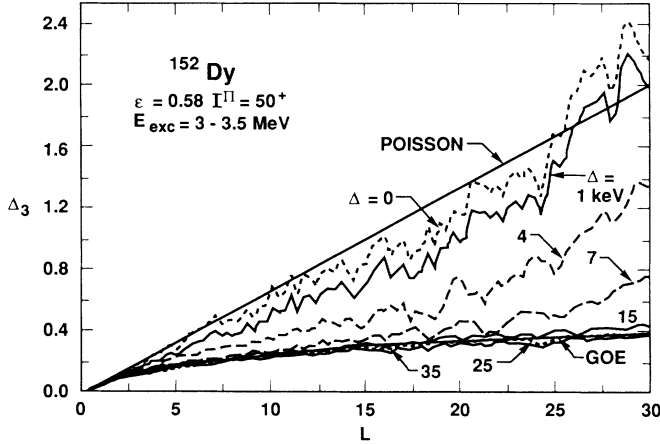


FIG. 3. Δ_3 statistics for different strengths Δ of the two-body force. The calculation has been performed for the superdeformed ^{152}Dy at $I^\pi = 50^+$ for rotational states in the excitation-energy interval 3–3.5 MeV above yrast (about 250 bands).

tion is given by Γ_μ . Correlations outside Γ_μ , or in terms of L , L values larger than $L_{\text{range}} \sim \bar{\rho}_{\text{tot}} \Gamma_\mu$, may thus be different than for smaller- L values. For the ^{152}Dy case we would expect a nongeneric behavior above $L_{\text{range}} \sim 0.3\Delta^2 \sim 4, 13$, and 61 for $\Delta = 4, 7$, and 15 keV, respectively. Tendencies for a nongeneric behavior may indeed be seen in Fig. 3 for the smaller values of Δ in the sense that the Δ_3 curves conserve the unperturbed behavior.

Different recipes exist for describing the spectrum properties of a mixed ordered and chaotic system; see, e.g., Ref. 11. Generally, it seems to be difficult to get a good description of mixed nearest-neighbor spacing distributions. Assuming a mixed spectrum the Δ_3 distribution becomes¹²

$$\Delta_3(L; q) = \Delta_3^{\text{Poisson}}[(1-q)L] + \Delta_3^{\text{GOE}}(qL), \quad (4)$$

exhibiting the limiting values $q=0$ and 1 for Poisson and GOE distributions, respectively. By comparing q values fitted from Eq. (4) with the classical phase-space part covered by chaotic trajectories, Hönig and Wintgen obtained a very good agreement for the hydrogen atom in a strong magnetic field.¹¹ We shall therefore also calculate here a mixing ratio by fitting the calculated Δ_3 curves with Eq. (4), and in Fig. 4 we show the q values corresponding to the distributions of Fig. 3. Note the smooth transition from Poisson to GOE at around $\Delta = 15$ keV for the considered energy interval, 3–3.5 MeV. In the normal-deformed ^{168}Yb the transition occurs around $\Delta = 15$ keV for the energy interval 1.5–2 MeV (cf. Fig. 2).

Next we shall study a dynamical property of the model, namely, how the strength function of the collective rotational decay fragments. By performing the above de-

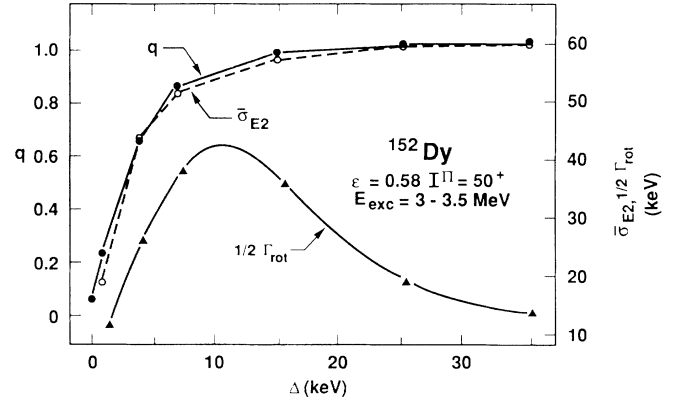


FIG. 4. As a function of the two-body coupling strength, three variables are shown: mixing parameter q between Poisson ($q=0$) and GOE ($q=1$) statistics (left-hand scale); average standard deviation of $E2$ strength function $\bar{\sigma}_{E2}$; and half-width of $E2$ strength function Γ_{rot} (right-hand scale).

scribed calculation at two consecutive spin values, I and $I-2$, the distribution of the reduced matrix elements for the $E2$ decay is calculated. Matrix elements between the unperturbed rotational states $|\mu, I\rangle$ are taken as $\langle \mu, I | \mu', I-2 \rangle \propto \delta_{\mu, \mu'}$. The rotational strength functions for each mother state in an energy interval are added, after they have been shifted to the same average transition energy. In Fig. 4 we show the average standard deviation $\bar{\sigma}_{E2}$ for the superdeformed ^{152}Dy for 50^+ states in the energy interval 3–3.5 MeV. $\bar{\sigma}_{E2}$ increases smoothly from 0 at $\Delta=0$ up to a saturated value of about 60 keV around $\Delta=15$ keV. Particularly, we note the extremely close correspondence between the dynamical property $\bar{\sigma}_{E2}$ and the chaoticity parameter q , obtained from the static spectra. (Also in Ref. 13 the onset of chaos was discussed to be related to a fragmentation of the transition strength.) A close correspondence between q and $\bar{\sigma}_{E2}$ is also seen in the calculations at other excitation-energy intervals in ^{152}Dy , as well as for ^{168}Yb .¹⁰ The saturated value of $\bar{\sigma}_{E2}$ in Fig. 4 is close to twice ($\Delta I=2$) the spread in rotational frequency $2\sigma_\omega$ shown in Fig. 2.

With an increasing value of Δ the eigenfunctions of (1) will contain a mixing of an increasing number of np - nh configurations. At $\Delta=0$ each wave function corresponds to a pure np - nh state with a given rotational frequency, but with increasing Δ , i.e., increasing degree of chaoticity q , more and more frequencies become involved. This means that the wave function of a typical mother state with spin I contains components with different moments of inertia, and a spreading arises in the corresponding $E2$ strength function ($I \rightarrow I-2$). At most the wave function can contain the full spread in rotational frequency σ_ω ; i.e., the spread in the $E2$ strength function saturates at $2\sigma_\omega$.

The shape of the strength function is found to change from Gaussian to Breit-Wigner form as Δ increases.

Therefore the half-width may change, although the standard deviation $\bar{\sigma}_{E2}$ stays constant. In Fig. 4 we show how this width Γ_{rot} first increases in accordance with $\bar{\sigma}_{E2}$ and then decreases. This phenomenon ("motional narrowing") has been predicted for the rotational strength function⁶ to occur for $\Gamma_{\mu} \gg 2\sigma_{\omega}$. With our microscopically calculated level density and spread in rotational frequency for the case shown in Fig. 4, we get $\Gamma_{\mu} = 2\sigma_{\omega}$ at $\Delta \approx 12$ keV, and motional narrowing is seen to set in already at this point. The predicted Δ dependence of the width in the region of motional narrowing,⁵ $\Gamma_{\text{rot}} = 2(2\sigma_{\omega})^2/\Gamma_{\mu} \approx 17500/\Delta^2$, agrees nicely with the microscopic calculation of Fig. 4. Note, however, that the onset of chaos and motional narrowing are not immediately correlated. Chaos sets in when $\Delta \approx \bar{d}_{2p-2h}$ while motional narrowing sets in when $\Delta \approx (\bar{d}_{2p-2h}\sigma_{\omega}/\pi)^{1/2}$.

It is to be noted that the widths shown in Fig. 4 relate to (the average) $E2$ fragmentation of *one* mother state. If the strength functions for each mother state are added without a shift to the same average transition energy, the standard deviation of this $E2$ strength function becomes approximately independent of Δ and equals $2\sigma_{\omega}$. Thus, to experimentally detect the *onset* of chaos one has to study a quantity sensitive to the widths of individual states as shown in Fig. 4. (In the chaotic regime the two strength functions become the same.) One possibility is to study correlations between two consecutive γ rays in an $E2$ cascade, $E_{\gamma 1}$ and $E_{\gamma 2}$ (γ - γ correlations). At low excitation energies (or small Δ) the width of the $E_{\gamma 1} - E_{\gamma 2}$ strength distribution is small since most transitions occur along well-defined rotational bands. In the two considered examples, ^{152}Dy at $E_{\text{exc}} = 3\text{--}3.5$ MeV and ^{168}Yb at $E_{\text{exc}} = 1.5\text{--}2$ MeV, the width of the γ - γ strength distribution increases from, respectively, 16 and 33 keV at $\Delta = 0$, to approximately 120 and 300 keV when chaos sets in ($\Delta \approx 15$ keV); i.e., the valley in the γ - γ plot has more or less disappeared. A more detailed discussion on these matters will be published elsewhere.¹⁰

In conclusion, we have utilized a "realistic" nuclear model to study the onset of chaos in rapidly rotating nuclei. GOE distributions ("quantum chaos") were found to smoothly set in as the strength of the two-body interaction Δ increases to a value around the average level distance between 2p-2h neighbors. Large shell effects in the onset of chaos were found. The dispersion in rotational frequency was found to increase approximately linear in angular momentum, and to be considerably smaller for the superdeformed ^{152}Dy than for the normal-deformed ^{168}Yb . We have addressed the question of how chaotic dynamics is related to a macroscopic quantum observable: It was found that the standard de-

viation of the collective rotational strength function behaves in the same way versus Δ as the mixing parameter q between chaotic and regular phase spaces. Finally, it was shown that the damping width may still change due to a change of the distribution function, and motional narrowing is obtained in the numerical calculation.

Discussions with T. Døssing are acknowledged. I thank the Joint Institute for Heavy Ion Research at Oak Ridge National Laboratory for kind hospitality. This work was supported by the Department of Energy under Contract No. DE-FG05-87 ER 40361, and the Swedish Natural Science Research Council.

(a) Present and permanent address.

¹G. Casati *et al.*, in *Stochastic Behavior in Classical Quantum Hamiltonian Systems*, edited by G. Casati and J. Ford, Lecture Notes in Physics Vol. 93 (Springer-Verlag, Berlin, 1977), p. 334.

²S. Adachi, M. Toda, and K. Ikeda, Phys. Rev. Lett. **61**, 659 (1988).

³Theoretical (in the semiclassical limit) [see M. V. Berry and M. Tabor, Proc. Roy. Soc. London A **356**, 375 (1977); M. V. Berry, Proc. Roy. Soc. London A **400**, 229 (1985); Nonlinearity **1**, 399 (1988)] as well as numerical [see, e.g., O. Bohigas and M.-J. Giannoni, in *Mathematical and Computational Methods in Nuclear Physics*, edited by J. S. Dehesa, J. M. G. Gomez, and A. Polls, Lecture Notes in Physics Vol. 209 (Springer-Verlag, Berlin, 1984), p. 1] studies indicate a generic behavior of (short-ranged) spectrum fluctuations: Poisson fluctuations when the corresponding classical system is ordered, and GOE fluctuations when it is chaotic (we only discuss systems which obey time-reversal symmetry). In this Letter we shall therefore by "quantum chaos" mean a quantum-mechanical system that shows GOE fluctuations.

⁴G. Andersson *et al.*, Nucl. Phys. A **268**, 205 (1976).

⁵S. Åberg, Phys. Scr. **25**, 23 (1982).

⁶B. Lauritzen, T. Døssing, and R. A. Broglia, Nucl. Phys. A **457**, 61 (1986).

⁷T. Guhr and H. A. Weidenmüller, Ann. Phys. (N.Y.) **193**, 472 (1989).

⁸Very similar results to those presented in this Letter are obtained with $V_2 = +\Delta$. This shows that the GOE behavior does not come from the randomness in the sign of the interaction, but rather from the drastic variation in matrix elements (from 0 to V_2), caused by the fact that the interaction is of the two-body type.

⁹Alternatively one could have required $\Gamma_{\mu}/\sigma_{\omega}$ to be constant. This would give $s = \Delta^2 E_{\text{exc}}^{5/4}$. Also due to shell effects (in ρ_{2p-2h}) the excitation-energy dependence may be slightly modified.

¹⁰S. Åberg (to be published).

¹¹A. Hönig and D. Wintgen, Phys. Rev. A **39**, 5642 (1989).

¹²T. A. Brody *et al.*, Rev. Mod. Phys. **53**, 385 (1981).

¹³T. H. Seligman, J. J. M. Verbaarschot, and H. A. Weidenmüller, Phys. Lett. **167B**, 365 (1986).